Article

Electronic Excitation Energies of ZnO Clusters

Jon M. Matxain, Jose M. Mercero, Joseph E. Fowler, and Jesus M. Ugalde

J. Am. Chem. Soc., **2003**, 125 (31), 9494-9499• DOI: 10.1021/ja0264504 • Publication Date (Web): 11 July 2003

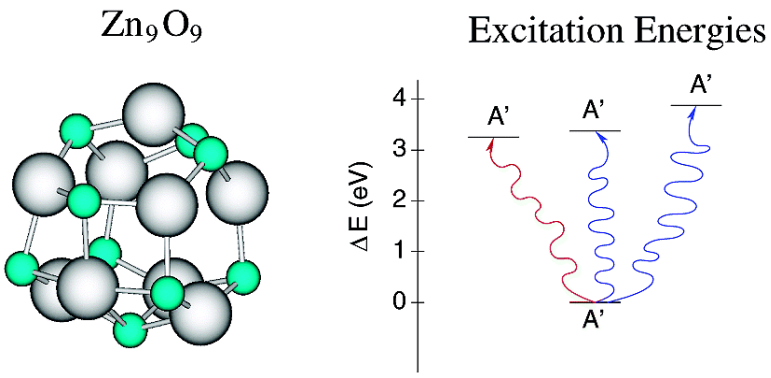

More About This Article

Additional resources and features associated with this article are available within the HTML version:

- Supporting Information
- Links to the 8 articles that cite this article, as of the time of this article download
- Access to high resolution figures
- Links to articles and content related to this article
- Copyright permission to reproduce figures and/or text from this article

View the Full Text HTML

J|A|C|S
ARTICLES
Published on Web 07/11/2003

Electronic Excitation Energies of Zn_iO_i Clusters

Jon M. Matxain,* Jose M. Mercero, Joseph E. Fowler, and Jesus M. Ugalde

Contribution from the Kimika Fakultatea, Euskal Herriko Unibertsitatea, P.K. 1072, 20018 Donostia, Euskadi, Spain

Received April 8, 2002; E-mail: pobmabej@sq.ehu.es

Abstract: Time-dependent density-functional theory (TDDFT) is used to study the excitation energies of the global minima of small Zn_iO_i clusters, $i = 1-15$. The relativistic compact effective core potentials and shared-exponent basis set of Stevens, Krauss, Basch, and Jasien (SKBJ), systematically enlarged with extra functions, were used throughout this work. In general, the calculated excitations occur from the nonbonding p orbitals of oxygen. These orbitals are perpendicular to the molecular plane in the case of the rings and normal to the spheroid surface for 3D clusters. The calculated excitation energies are larger for ringlike clusters as compared to 3D clusters, with the excitation energies of the latter structures lying close to the visible spectrum. The difference between Kohn−Sham eigenvalues of the orbitals involved in the electronic excitations studied have also been compared to the TDDFT results of the corresponding excitations for two approximate density functionals, that is, MPW1PW91 and B3LYP, the latter being more accurate. Moreover, they approach the TDDFT value as the cluster size increases. Therefore, this might be a practical method for estimating excitation energies of large Zn_iO_i clusters.

1. Introduction

Semiconductors have been and are of great importance in technology development. Computer revolution and other technological devices have been and are in rapid development basically due to improved semiconductor materials. Some of these materials are the II-VI compounds, the interest of which has increased notably due to their paramount technological potential. Applications such as photovoltaic solar cells,[1−10] optical sensitizers,[11] photocatalysts,[12,13] or quantum devices[14] have led to extensive investigation. Many theoretical studies have been reported concerning the bulk electronic structure of these compound semiconductors.[15−22] The band gaps of these compounds make them especially interesting for photovoltaic solar cells. A typical solar cell is composed of a p-type and an n-type semiconductor. The p-type material is called absorber, and the n-type material is called window. Obviously, the absorption mainly occurs in the absorber, but the window material is also very important. The electrons excited in the absorber are stored in the window material, and thus a potential difference is created between the window and the absorber, which is indispensable for generating electricity. The sun irradiates most of its energy within the visible spectrum, the range of which is very narrow (1.75−3 eV). Therefore, a good material for its use as an absorber in a solar cell must have band gaps close to or within the range of energies given above. These band gaps for the window materials are larger. The II-VI compound semiconductors have these properties. The band gaps go from 1.45 eV for CdTe to 3.66 eV for ZnS, and all of these compounds present either p- or n-type semiconduction.[1] Therefore, these materials are ideally suited for use in solar cells.

The fact that cluster and nanoparticle characterization is becoming technologically possible opens new possibilities in the development of materials which could improve the efficiency of the cells. Besides, important developments concerning nanoelectronics and nanowires[23−26] are in rapid evolution. New nanocompounds that could be useful in a broader way than their bulk counterparts might be created.[27−31]

(1) Chu, T. L.; Chu, S. S. *Solid-State Electron.* **1995**, *38*, 533.
(2) Halliday, D. P.; Eggleston, J. M.; Durose, K. *Thin Solid Films* **1998**, *322*, 314.
(3) Yamamoto, T.; Toyama, T.; Okamoto, H. *Jpn. J. Appl. Phys.* **1998**, *37*, L916.
(4) Lee, J. H.; Lee, H. Y.; Park, Y. K.; Shin, S. H.; Park, K. J. *Jpn. J. Appl. Phys.* **1998**, *37*, 3357.
(5) Singh, V. P.; McClure, J. C.; Lush, G. B.; Wang, W.; Wang, X.; Thompson, G. W.; Clark, E. *Sol. Energy Mater. Sol. Cells* **1999**, *59*, 145.
(6) Burgelman, M.; Nollet, P.; Degrave, S. *Appl. Phys. A* **1999**, *69*, 149.
(7) Durose, K.; Edwards, P. R.; Halliday, D. P. *J. Crys. Growth* **1999**, *197*, 733.
(8) Contreras, G.; Vigil, O.; Ortega, M.; Morales, A.; Vidal, J.; Albor, M. L. *Thin Solid Films* **2000**, *361−362*, 378.
(9) Chakrabarti, R.; Dutta, J.; Bandyopadhyay, S.; Bhattacharyya, D.; Chaudhuri, S.; Pal, A. K. *Sol. Energy Mater. Sol. Cells* **2000**, *61*, 113.
(10) Edwards, P. R.; Galloway, S. A.; Durose, K. *Thin Solid Films* **2000**, *361−362*, 364.
(11) Sebastian, P. J.; Ocampo, M. *Sol. Energy Mater. Sol. Cells* **1996**, *44*, 1.
(12) Hoffman, A. J.; Mills, G.; Yee, H.; Hoffmann, M. R. *J. Phys. Chem.* **1992**, *96*, 5546.
(13) Kuwabata, S.; Nishida, K.; Tsuda, R.; Inoue, H.; Yoneyama, H. *J. Electrochem. Soc.* **1994**, *141*, 1498.
(14) Corcoran, E. *Sci. Am.* **1990**, *263*, 74.
(15) Schroer, P.; Kruger, P.; Pollmann, J. *Phys. Rev. B* **1993**, *47*, 6971.
(16) Schroer, P.; Kruger, P.; Pollmann, J. *Phys. Rev. B* **1993**, *48*, 18264.
(17) Schroer, P.; Kruger, P.; Pollmann, J. *Phys. Rev. B* **1994**, *49*, 17092.
(18) Vogel, D.; Kruger P.; Pollmann, J. *Phys. Rev. B* **1995**, *52*, 14316.
(19) Pollmann, J.; Kruger, P.; Rohlfing, M.; Sabisch, M.; Vogel, D. *Appl. Surf. Sci.* **1996**, *104/105*, 1.
(20) Vogel, D.; Kruger, P.; Pollmann, J. *Phys. Rev. B* **1996**, *54*, 5495.
(21) Muilu, J.; Pakkanen, T. A. *Surf. Sci.* **1996**, *364*, 439.
(22) Muilu, J.; Pakkanen, T. A. *Phys. Rev. B* **1994**, *49*, 11185.
(23) Zach, M. P.; Ng, K. H.; Penner, R. M. *Science* **2000**, *290*, 2120.
(24) Joachim, C.; Gimzewski, J. K.; Aviram, A. *Nature* **2000**, *408*, 541.
(25) Chadwick, A. V. *Nature* **2000**, *408*, 925.
(26) Sata, N.; Eberman, K.; Eberl, K.; Maier, J. *Nature* **2000**, *408*, 946.
(27) Craighead, H. G. *Science* **2000**, *290*, 1532.
(28) Quake, S. R.; Schrerer, A. *Science* **2000**, *290*, 1536.
(29) Jager, E. W. H.; Smela, E.; Inganäs, O. *Science* **2000**, *290*, 1540.

10.1021/ja0264504 CCC: $25.00

Recently, absorption energies of ultrasmall nanoparticles of zinc oxide have been measured. Thus, nanoparticles of 4 nm diameter absorb at 3.81 eV, and nanoparticles of 8.5 nm diameter absorb at 3.65 eV.[32] Smaller nanoparticles, with a diameter of 2.5 nm, have also been recently synthesized.[33] These nanoparticles are obtained by quenching the crystal growth by the adsorption of octadienol. The absorption energies of these nanoparticles converge to the bulk band gap, which is 3.2 eV, as the size increases. In this work, the diameter of the largest spheroid we have studied is 0.68 nm. Moreover, the coordination number (which is the number of atoms each atom is bonded to) of these spheroids is three, while it is "claimed" to be four for the nanoparticles found experimentally.[33] Therefore, the present work is well-suited to ascertain the influence of the distinct chemical environment of the cluster, as compared to nanoparticles, on the excitation energies.

Our goal is to calculate the excitation energies of Zn_iO_i global minima, $i = 1-15$, where ring structures were found to be the global minima for $i \leq 7$, and spheroids were found to be for $i > 7$.[34] Previous work on the excitation energies of Zn_iS_i clusters[35,36] has shown that TDDFT provided more accurate results than CIS and that TDDFT is a valid tool for calculating the excitation energies of II-VI compounds. Additional reports on the reliability of TDDFT have appeared recently.[37,38] Recall that, in TDDFT, the excitation energies are calculated from the poles of the frequency-dependent polarizability, and their corresponding oscillator strengths are calculated from the residues.

2. Methods

As in the case of Zn_iO_i clusters, $i = 1-9$,[34] all geometries of Zn_iO_i clusters, $i = 10-15$, were fully optimized using the hybrid[39] Becke 3 Lee−Yang−Perdew (B3LYP) gradient-corrected approximate density-functional procedure.[40−42] Harmonic vibrational frequencies were determined by analytical differentiation of gradients.

TDDFT[43−48] calculations have been performed for the excitation energies of geometry-optimized Zn_iO_i clusters. As in the case of the calculation of the excitation energies of Zn_iS_i clusters,[35,36] the hybrid Becke-style one parameter functional using modified Perdew−Wang exchange and Perdew−Wang 91 correlation (MPW1PW91)[49] was used.

Table 1. Extra Functions Added to the SKBJ Basis

	Zn			O		
	α	*d*	*d*	α	*d*	*d*
sp	0.017900	1.00	1.00	0.066667	0.28472	0.30727
sp	0.005967	1.00	1.00	0.022222	0.28472	0.30727
sp	0.001989	1.00	1.00	0.007407	0.28472	0.30727
d	0.3264	1.00		0.85	1.00	
d	0.1088	1.00		0.283333	1.00	
d	0.03627	1.00		0.094444	1.00	
d	0.01209	1.00		0.031481	1.00	
f	3.1109	1.00		0.6	1.00	
f	1.037	1.00		0.2	1.00	
f	0.3457	1.00		0.066667	1.00	
f	0.1152	1.00		0.022222	1.00	

The relativistic compact effective core potentials and shared-exponent basis set[50] of Stevens, Krauss, Basch, and Jasien (SKBJ) were used throughout this study, with the Zn d electrons treated as valence electrons. For the geometry optimizations, an extra d function was added on Zn, as described in ref 34. To analyze the influence of the basis set size on the calculated excitation energies, extra functions were systematically added to SKBJ to a maximum of extra 3sp4d4f functions. These functions were systematically generated by dividing the exponent of the previous function by three. The final exponents are given in Table 1. These larger basis sets are labeled according to the number of added functions. Thus, for instance, the largest basis set used in this work is denoted as SKBJ(3sp4d4f).

3. Results and Discussion

In section 3.1, the structures of Zn_iO_i spheroids, $i = 10-15$, are described, while in section 3.2, the excitation energies of these structures and previously characterized global minima are given. In section 3.2.1, the basis set influence is discussed for small Zn_iO_i clusters, $i = 1-3$. In section 3.2.2, the obtained TDDFT excitation energies of Zn_iO_i clusters, $i = 1-15$, are fully discussed. Finally, in section 3.2.3, the reliability of the Kohn−Sham eigenvalues is discussed.

In ref 34, ringlike structures were found to be the global minima for Zn_iO_i clusters, $i \leq 7$, and spheroids were found to be for $i > 7$. Rings are depicted in Figure 1, and spheroids are shown in Figure 2. These spheroidal structures are built by a constant number of squares, 6, and an increasing number of hexagons, as the cluster size increases, as can be observed in Table 2.

It has been demonstrated elsewhere[52] that many cluster properties, in accordance with the liquid drop model, lie within lines when plotted versus $i^{-1/3}$, where i is the number of ZnO units. The cohesive energy

$$E_f = \frac{iE_{Zn} + iE_O - E_{Zn_iO_i}}{i} \quad (1)$$

(30) Paiella, R.; Capasso, F.; Gmachi, C.; Sivco, D. L.; Baillargeon, J. N.; Hutchinson, A. L.; Cho, A. Y.; Liu, H. C. *Science* **2000**, *290*, 1739.
(31) Suenaga, K.; Tencé, M.; Mory, C.; Colliex, C.; Kato, H.; Okazaki, T.; Shinohara, H.; Hirahara, K.; Bandow, S.; Lijima, S. *Science* **2000**, *290*, 2280.
(32) Mahamuni, S.; Borgohain, K.; Bendre, B. S.; Leppert, V. J.; Risbud, S. H. *J. Appl. Phys.* **1999**, *85*, 2861.
(33) Pesika, N. S.; Hu, Z.; Stebe, K. J.; Searson, P. C. *J. Phys. Chem. B* **2002**, *106*, 6985.
(34) Matxain, J. M.; Fowler, J. E.; Ugalde, J. M. *Phys. Rev. A* **2000**, *62*, 553.
(35) Matxain, J. M.; Irigoras, A.; Fowler, J. E.; Ugalde, J. M. *Phys. Rev. A* **2000**, *63*, 013202.
(36) Matxain, J. M.; Irigoras, A.; Fowler, J. E.; Ugalde, J. M. *Phys. Rev. A* **2001**, *64*, 013201.
(37) Hirata, S.; Head-Gordon, M. *Chem. Phys. Lett.* **1999**, *302*, 375.
(38) Wiberg, K. B.; Stratmann, R. E.; Frisch, M. J. *Chem. Phys. Lett.* **1998**, *297*, 60.
(39) Becke, A. D. *J. Chem. Phys.* **1993**, *98*, 5648.
(40) Hohemberg, P.; Kohn, W. *Phys. Rev.* **1964**, *136*, 3864.
(41) Lee, C.; Yang W.; Parr, R. G. *Phys. Rev. B* **1988**, *37*, 785.
(42) Becke, A. D. *Phys. Rev. A* **1988**, *38*, 3098.
(43) Runge, E.; Gross, E. K. U. *Phys. Rev. Lett.* **1984**, *52*, 997.
(44) Gross, E. K. U.; Kohn, W. *Phys. Rev. Lett.* **1985**, *55*, 2850.
(45) Mearn, D.; Kohn, W. *Phys. Rev. A* **1987**, *35*, 4796.
(46) Stratmann, R. E.; Scuseria, G. E.; Frisch, M. J. *J. Chem. Phys.* **1998**, *109*, 8218.
(47) Bauernschmitt, R.; Ahlrichs, R. *Chem. Phys. Lett.* **1996**, *256*, 454.
(48) Casida, M. E.; Jamorski, C.; Casida, K. C.; Salahub, D. R. *J. Chem. Phys.* **1998**, *108*, 4439.
(49) Adamo, C.; Barone, V. *Chem. Phys. Lett.* **1997**, *274*, 242.
(50) Stevens, W. J.; Krauss, M.; Basch H.; Jasien, P. G. *Can. J. Chem.* **1990**, *70*, 612.
(51) Frisch, M. J.; Trucks, G. W.; Schlegel, H. B.; Scuseria, G. E.; Robb, M. A.; Cheeseman, J. R.; Zakrzewski, V. G.; Montgomery, J. A., Jr.; Stratmann, R. E.; Burant, J. C.; Dapprich, S.; Millam, J. M.; Daniels, A. D.; Kudin, K. N.; Strain, M. C.; Farkas, O.; Tomasi, J.; Barone, V.; Cossi, M.; Cammi, R.; Mennucci, B.; Pomelli, C.; Adamo, C.; Clifford, S.; Ochterski, J.; Petersson, G. A.; Ayala, P. Y.; Cui, Q.; Morokuma, K.; Malick, D. K.; Rabuck, A. D.; Raghavachari, K.; Foresman, J. B.; Cioslowski, J.; Ortiz, J. V.; Stefanov, B. B.; Liu, G.; Liashenko, A.; Piskorz, P.; Komaromi, I.; Gomperts, R.; Martin, R. L.; Fox, D. J.; Keith, T.; Al-Laham, M. A.; Peng, C. Y.; Nanayakkara, A.; Gonzalez, C.; Challacombe, M.; Gill, P. M. W.; Johnson, B. G.; Chen, W.; Wong, M. W.; Andres, J. L.; Head-Gordon, M.; Replogle, E. S.; Pople, J. A. *Gaussian 98*, revision A.7; Gaussian, Inc.: Pittsburgh, PA, 1998.

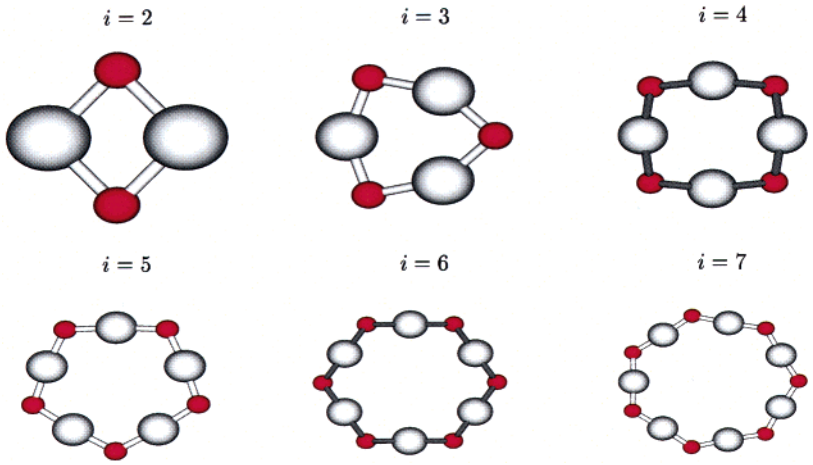

Figure 1. Calculated ring structures of Zn_iO_i, $i = 2-7$; red, smaller atoms are those of O.

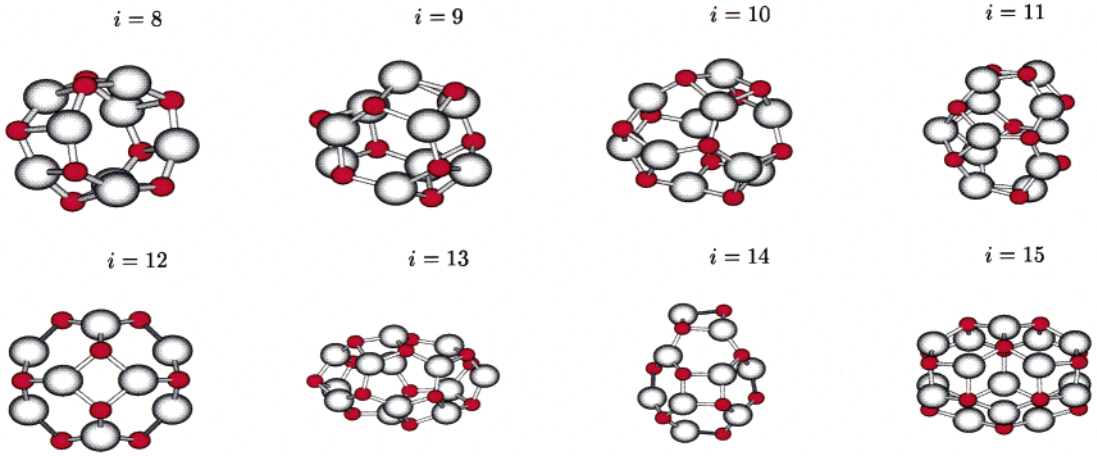

Figure 2. Calculated spheroids for Zn_iO_i, $i = 8-15$.

Table 2. Structural Pattern of Spheroid Zn_iO_i Clusters

	Zn_8O_8	Zn_9O_9	$Zn_{10}O_{10}$	$Zn_{11}O_{11}$	$Zn_{12}O_{12}$	$Zn_{13}O_{13}$	$Zn_{14}O_{14}$	$Zn_{15}O_{15}$
hexagons	4	5	6	7	8	9	10	11
squares	6	6	6	6	6	6	6	6

is one of these properties. It has been observed both theoretically and experimentally for Si[53] that clusters belonging to the same family lie within a line. The family lying above is the most stable family in that cluster size range.

The cohesive energies of these Zn_iO_i spheroids, $i = 8-15$, are plotted versus $i^{-1/3}$ in Figure 3 and may be consulted in Table 1 of the Supporting Information. Fitting a line to these points, and extrapolating it to $i^{-1/3} = 0$, the theoretical value for the cohesive energy of the bulk can be obtained. The predicted cohesive energy is 706 kJ/mol, and the experimental value, which is calculated according to the CODATA data[54] by eq 2,

$$E_{f,exp} = |\Delta H^\circ_f(ZnO) - \Delta H^\circ_f(Zn) - \Delta H^\circ_f(O)| - RT \quad (2)$$

is 718 kJ/mol. The theoretical and experimental values agree well, although the clusters used in this extrapolation have a coordination number of three and not four like the bulk. This

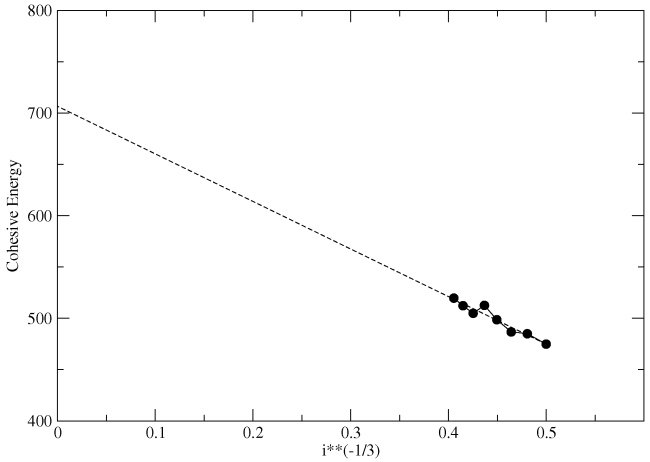

Figure 3. Cohesive energies of the Zn_iO_i clusters versus $i^{-1/3}$, in kJ/mol.

fit is consistent with our prediction of the global minima structures, because there is no space above this line in this cluster size region for another cluster family. Nevertheless, this family, or families, is expected to be dominant in the region of larger cluster sizes.

The second difference in energy is a measurement of the stability of the structures. It can be calculated according to

$$\Delta_2 E(Zn_iO_i) = E(Zn_{i+1}O_{i+1}) + E(Zn_{i-1}O_{i-1}) - 2E(Zn_iO_i) \quad (3)$$

(52) Jortner, J. *Z. Phys. D: At., Mol. Clusters* **1992**, *24*, 247.
(53) Hartke, B. *Angew. Chem., Int. Ed.* **2000**, *41*, 1468 and references therein.
(54) Lide, D. R., Ed. *Handbook of Chemistry and Physics*, 79th ed.; CRC Press: Boca Raton, FL, 1998−1999; pp 5−24.

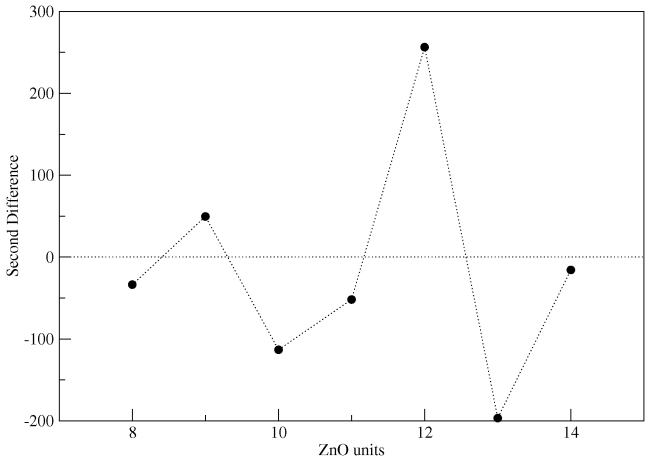

Figure 4. Second differences of the total energies of Zn_iO_i spheroidal clusters, $i = 8-14$, in kJ/mol.

and positive values of it correspond to stable structures. These stable structures are associated with electronic shell closure within the jellium model.[55] This quantity is also often used as a measure of local stability. The graph of $\Delta_2E(Zn_iO_i)$ shown in Figure 4 displays maxima at $i = 12$ and $i = 9$. The latter corresponds to the ellipsoidal shell closure at 54 electrons.[56]

3.2. TDDFT Excitation Energies of Zn_iO_i Clusters. 3.2.1. Basis Set Influence on the TDDFT Excitation Energies. In this section, the calculated TDDFT excitation energies for Zn_iO_i global minima, $i = 1-3$, are shown. The SKBJ shared exponent basis set was systematically enlarged to find the most proper basis set. Only the Zn_1O_1 case is fully discussed, because the conclusions are similar for the rest.

In Table 3, the TDDFT excitation energies of Zn_1O_1 are shown. In a rapid glance, it may be observed that the addition of extra functions to the SKBJ basis changes significantly the final result. For the sake of brevity, we will focus the discussion on the calculated excitation energies, with different basis sets, for the $^1\Pi$ state. Observe that the basis-set size effect is similar in the $^1\Sigma$ state, and therefore only the small differences will be pointed out. The influence of extra sp, d, and f functions is analyzed separately.

To study the influence of extra sp functions, the results of SKBJ(1d), SKBJ(1sp1d), and SKBJ(2sp1d) are compared, which are 0.7637, 0.7877, and 0.7875 eV, respectively. It is seen that while the addition of extra s and p functions to SKBJ(1d) changes the resulting excitation energy significantly, more s and p additions do not. The same behavior is observed comparing the SKBJ(1d1f), SKBJ(1sp1d1f), and SKBJ(2sp1d1f) results, that is, 0.8181, 0.8396, and 0.8394 eV, respectively. We henceforth conclude that one extra sp function seems a good choice at this point.

Analyzing the influence of extra d functions, we see that the addition of three extra d functions is not necessary, as follows from the results of SKBJ(1sp1d), SKBJ(1sp2d), and SKBJ(1sp3d), which are 0.7877, 0.7801, and 0.7786 eV, respectively. The results obtained adding two and three extra d functions do not differ significantly, but they do in a considerable manner when adding only one. Therefore, two d functions were added.

Table 3. TDDFT Results for Zn_1O_1[a]

	$^1\Pi$		$^1\Sigma$	
SKBJ +	ΔE	f	ΔE	f
1d	0.7637	0.0020	3.8173	0.1007
2d	0.7592	0.0018	3.8227	0.1043
3d	0.7801	0.0017	3.8359	0.1130
1sp1d	0.7877	0.0019	3.8180	0.1129
2sp1d	0.7875	0.0019	3.8181	0.1135
1sp2d	0.7801	0.0018	3.8237	0.1126
2sp2d	0.7804	0.0018	3.8238	0.1128
1sp3d	0.7786	0.0018	3.8225	0.1128
2sp3d	0.7771	0.0018	3.8210	0.1128
1d1f	0.8181	0.0022	3.8000	0.0996
1sp1d1f	0.8396	0.0021	3.7999	0.1116
1sp2d1f	0.8351	0.0020	3.8033	0.1128
1sp3d1f	0.8339	0.0020	3.8025	0.1128
1sp2d2f	0.8629	0.0021	3.7928	0.1106
1sp2d3f	0.8719	0.0021	3.7972	0.1099
2sp1d1f	0.8394	0.0021	3.7999	0.1121
2sp1d2f	0.8671	0.0022	3.7887	0.1104
2sp1d3f	0.8805	0.0023	3.7957	0.1086
2sp2d1f	0.8352	0.0020	3.8033	0.1130
2sp2d2f	0.8630	0.0021	3.7926	0.1107
2sp2d3f	0.8718	0.0021	3.7963	0.1100
2sp3d1f	0.8328	0.0020	3.8011	0.1129
2sp3d2f	0.8618	0.0021	3.7924	0.1107
2sp3d3f	0.8726	0.0021	3.7954	0.1097
3sp4d4f	0.8743	0.0021	3.7951	0.1098

[a] ΔE is the excitation energy (eV), and f is the oscillator strength.

Finally, the influence of extra f functions is analyzed. For the $^1\Pi$ state, we focus now on the SKBJ(2sp2d), SKBJ(2sp2d1f), SKBJ(2sp2d2f), and SKBJ(2sp2d3f) excitation energies, 0.7804, 0.8352, 0.8630, and 0.8718 eV, respectively. This last value still diverges considerably from that with only two extra f functions. However, when it is compared to the SKBJ(2sp3d3f) ΔE, which is 0.8726 eV, and to the SKBJ(2sp3d3f) ΔE, which is 0.8743, convergence is achieved. Therefore, three extra f functions are necessary. Consequently, SKBJ(1sp2d3f) is the smallest basis set yielding good results.

In Tables 2 and 3 of the Supporting Information, the results for Zn_2O_2 and Zn_3O_3 are given, where it is also seen that the SKBJ(1sp2d3f) basis set is the smallest one yielding good results. It seems logical then to choose SKBJ(1sp2d3f) for further calculations. However, for clusters as big as $i = 6$, the size of the basis set makes the calculations prohibitive. Henceforth, the smaller SKBJ(d) basis set was chosen for these larger clusters, while calculations with both SKBJ(1sp2d3f) and SKBJ(d) basis sets were performed for smaller clusters, $i \leq 5$. This allows us to asses the performance of the smaller basis set and consequently to highlight the limitations of the SKBJ(d) basis set with respect to SKBJ(1sp2d3f). In Table 4, the SKBJ(d) and SKBJ(1sp2d3f) excitation energies and oscillator strengths, along with the differences between them, of the structures shown in Figure 1 are given. Having a look at these differences, one may observe that although they are important for small clusters, $i = 1-3$, they are not very large for the rest. The largest difference in the excitation energy is 0.22 eV for the $^1A_g \rightarrow {}^1B_{1g}$ transition in Zn_2O_2, which represents more than 10% of the total excitation energy. Nevertheless, in the case of Zn_3O_3, the differences are reduced to 3−4% of the total energy, and to less than 1% for Zn_5O_5. Therefore, the SKBJ(d) results for larger clusters are expected to be reasonably accurate. A similar conclusion was obtained from the data on Zn_iS_i clusters.[36]

(55) Knight, W. D.; Clemenger, K.; de Heer, W. A.; Saunders, W. A.; Chou, M. Y.; Cohen, M. L. *Phys. Rev. Lett.* **1984**, *52*, 2141.
(56) Clemenger, K. *Phys. Rev. B* **1984**, *32*, 1359.

Table 4. SKBJ(d) and SKBJ(1sp2d2f) Excitation Energies (eV) and Oscillator Strengths of Zn_iO_i, $i = 1-5$[a]

		transition		SKBJ(d)		SKBJ(1sp2d3f)			
	val. conf.	orbitals	states	ΔE	f	ΔE	f	$\Delta(\Delta E)$	Δf
Zn_1O_1	$2\delta^2 4\sigma^2 5\sigma^2 5\pi^4$	$5\pi \rightarrow 6\sigma$	$^1\Sigma \rightarrow {}^1\Pi$	0.76	0.002	0.87	0.002	0.11	0
	LUMO: 6σ	$5\sigma \rightarrow 6\sigma$	$^1\Sigma \rightarrow {}^1\Sigma$	3.82	0.101	3.80	0.110	0.02	0.009
Zn_2O_2	$5b_{1u}{}^2 3b_{3g}{}^2 3_{3u}b^2 2b_{1g}{}^2 4b_{2u}{}^2$	$2b_{1g} \rightarrow 7a_g$	$^1A_g \rightarrow {}^1B_{1g}$	1.70	forbidden	1.92	forbidden	0.22	
	LUMO: $7a_g$	$4b_{2u} \rightarrow 7a_g$	$^1A_g \rightarrow {}^1B_{2u}$	1.92	0.009	2.08	0.010	0.16	0.001
		$3b_{3u} \rightarrow 7a_g$	$^1A_g \rightarrow {}^1B_{3u}$	2.71	0.024	2.86	0.023	0.15	0.001
Zn_3O_3	$6b_1{}^2 15a_1{}^2 12b_2{}^2 5a_2{}^2 7b_1{}^2$	$5a_2 \rightarrow 16a_1$	$^1A_1 \rightarrow {}^1A_2$	3.58	forbidden	3.67	forbidden	0.09	
	LUMO: $16a_1$	$7b_1 \rightarrow 16a_1$	$^1A_1 \rightarrow {}^1B_1$	3.58	forbidden	3.67	forbidden	0.09	
		$6b_1 \rightarrow 16a_1$	$^1A_1 \rightarrow {}^1B_1$	4.56	0.067	4.62	0.064	0.06	0.003
Zn_4O_4	$18e_u{}^2 7e_g{}^2 8e_g{}^2 4b_{2g}{}^2 2b_{1u}{}^2$	$2b_{1u} \rightarrow 7a_{1g}$	$^1A_1 \rightarrow {}^1B_{1u}$	3.78	forbidden	3.83	forbidden	0.05	
	LUMO: $7a_{1g}$	$3a_{2u} \rightarrow 7a_{1g}$	$^1A_{1g} \rightarrow {}^1A_{2u}$	5.17	0.095	5.19	0.084	0.02	0.011
		$18e_u \rightarrow 7a_{1g}$	$^1A_{1g} \rightarrow {}^1E_u$	5.24	0.111	5.24	0.110	0	0.001
Zn_5O_5	$28a''^2 34a'^2 29a''^2 30a''^2 35a'^2$	$35a' \rightarrow 36a'$	$^1A' \rightarrow {}^1A'$	4.00	forbidden	4.02	forbidden	0.02	
	LUMO: $36a'$	$32a' \rightarrow 36a'$	$^1A' \rightarrow {}^1A'$	5.27	0.106	5.28	0.091	0.01	0.015
		$31a' \rightarrow 36a'$	$^1A' \rightarrow {}^1A'$	5.60	0.164	5.57	0.157	0.03	0.007

[a] $\Delta(\Delta E)$ is the difference between SKBJ(1sp2d3f) ΔE and SKBJ(d) ΔE, similarly for Δf.

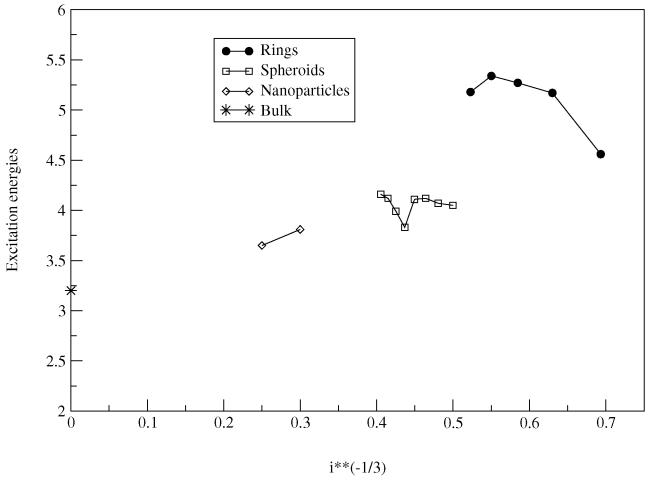

Figure 5. Excitation energies of the Zn_iO_i clusters, nanoparticles, and bulk, in eV.

3.2.2. TDDFT Excitation Energies of Small Zn_iO_i Clusters, $i = 1-15$. The range of the excitations we are interested in lie within the visible spectrum (1.75−3 eV) and close-UV (3−5 eV). The complete data set is given in Table 4 of the Supporting Information. In Figure 5, the excitation energies of the transitions having the largest oscillator strengths are depicted, along with the experimental data corresponding to nanocrystals[32] and bulk, versus the inverse of the cubic root of i, that is, $i^{-1/3}$. The range of $i^{-1/3}$ goes from 1 for Zn_1O_1 to 0 for the bulk. The change of the structure of the global minima, from ringlike structures for $i \leq 7$ to 3D spheroids for $i \geq 8$, has dramatic consequences in the calculated excitation energies. We observe that the excitation energies are near 5 eV and larger for $i = 3-7$. This value is drastically reduced by more than 1 eV for $i \geq 8$. The obtained values are around 4 eV for $i = 8-15$.

In all cases, the transitions occur from the nonbonding p orbitals of O to the LUMO, which correspond to virtual sp hybrids of Zn. In the ring structures, these orbitals lie perpendicular to the ring plane, while in the 3D case, they lie perpendicular to the spheroid's surface. This situation was also found for Zn_iS_i clusters.[36] The excitation energies of the 3D clusters lie close to those found experimentally for small nanocrystals. For instance, the excitation energies of a nanostructure of 4 nm of diameter are 3.8 eV.[32] The structure of these small nanocrystals is assumed to be bulklike by the authors. However, our calculations show a remarkable agreement between their excitation energies (∼3.8 eV) within that of $Zn_{12}O_{12}$ (3.83 eV), our most spherical and stable 3D cluster. This similarity pinpoints the fact that surface reconstruction might occur in small nanocrystals. Similar phenomena have been recently reported for diamond nanoparticles,[57] for which evidence of fullerene-like surface reconstruction yielding a new family of carbon clusters, having a diamond core of a few nanometers and a fullerene-like surface structure, has been found. ZnO nanoparticles might also undergo a similar process to end up with a small wurzite-like core and a surface with a pattern the same as that described earlier for $Zn_{12}O_{12}$. Analysis of the preedge signal of the X-ray absorption spectra of the small ZnO nanocrystals would show peaks indicating the presence of squares and hexagons on the reconstructed surface of the nanoparticle. Hence, these experiments are crucial in validating our structural model for small ZnO nanocrystals.

3.2.3. Excitation Energies Calculated as Kohn−Sham Eigenvalue Differences. The problem of the reliability of orbital eigenvalues within DFT is a topic of great controversy.[58] Indeed, recent experimental evidence has been given by Brion et al.[59] in support of the legitimacy of the Kohn−Sham orbitals to account for the features of their electron momentum spectroscopy (EMS) measurements on selected small molecules. However, the question of whether the eigenenergies of the virtual Kohn−Sham orbitals are reliable enough as to estimate excitation energies remains open. However, it has been recently demonstrated that, within the exact exchange-correlation potential theory, the calculated excitation energies as obtained from the Kohn−Sham orbital eigenenergies are very reliable.[60] Nevertheless, in real problems, exact correlation potentials are not available, and one has to deal with approximate exchange-correlation functionals. In this section, we estimate the excitation energies using the Kohn−Sham eigenvalues, as calculated from the B3LYP and MPW1PW91 approximate exchange-correlation potentials (see Table 5). These functionals were chosen because of their great usability. In particular, B3LYP is becoming a standard for geometry optimizations, and MPW1PW91 is one of the most employed approximate exchange-correlation functionals for the calculation of electronic excitation energies.

(57) Raty, J. Y.; Galli, G.; Bostedt, C.; van Buuren, T. W.; Terminello, L. J. *Phys. Rev. Lett.* **2003**, *90*, 7401.
(58) Tozer, D. J.; Handy, N. C. *J. Chem. Phys.* **1998**, *200*, 10180.
(59) Feng, R.; Sakai, Y.; Zheng, Y.; Cooper, G.; Brion, C. E. *Chem. Phys.* **2000**, *260*, 29.
(60) Savin, A.; Umrigar C. J.; Gonze, X. *Chem. Phys. Lett.* **1998**, 288, 391.

Table 5. Excitation Energies Calculated with TDDFT ($\Delta E(1)$), MPW1PW91 Kohn−Sham Orbital Differences ($\Delta E(2)$), and B3LYP Kohn−Sham Orbital Differences ($\Delta E(3)$)[a]

	$\Delta E(1)$	$\Delta E(2)$	D1	$\Delta E(3)$	D2		$\Delta E(1)$	$\Delta E(2)$	D1	$\Delta E(3)$	D2
Zn_1O_1	0.87	2.97	2.10	2.49	1.62	Zn_9O_9	3.20	4.19	0.99	3.62	0.42
	3.80	4.49	0.69	4.08	0.28		3.88	4.87	0.99	4.29	0.41
							4.07	5.02	0.95	4.45	0.38
Zn_2O_2	1.92	3.42	1.50	2.67	0.75	$Zn_{10}O_{10}$	3.14	4.09	0.93	3.53	0.39
	2.08	3.29	1.21	2.59	0.51		3.73	4.71	0.98	4.14	0.41
	2.86	4.29	1.43	3.58	0.72		4.12	5.10	0.98	4.51	0.39
Zn_3O_3	3.66	5.06	1.40	4.37	0.71	$Zn_{11}O_{11}$	3.23	4.18	0.95	3.61	0.38
	3.67	5.06	1.39	4.37	0.70		3.75	4.71	0.96	4.14	0.39
	4.62	5.97	1.35	5.29	0.67		4.11	5.06	0.95	4.47	0.36
Zn_4O_4	3.83	5.21	1.38	4.61	0.78	$Zn_{12}O_{12}$	3.72	4.69	0.97	4.11	0.39
	5.19	6.51	1.32	5.93	0.74		3.83	4.77	0.94	4.20	0.37
	5.24	6.39	1.15	5.82	0.58		4.16	5.17	1.01	4.57	0.41
Zn_5O_5	4.02	5.31	1.29	4.76	0.74	$Zn_{13}O_{13}$	3.24	4.13	0.89	3.58	0.34
	5.28	6.53	1.25	5.98	0.70		3.72	4.65	0.93	4.08	0.36
	5.57	6.69	1.12	6.15	0.58		3.99	4.86	0.87	4.29	0.30
Zn_6O_6	3.96	5.19	1.23	4.63	0.67	$Zn_{14}O_{14}$	3.27	4.18	0.91	3.63	0.36
	4.69	5.63	0.94	5.07	0.38		3.71	4.62	0.91	4.07	0.36
	5.34	6.54	1.20	5.99	0.65		4.12	4.97	0.85	4.41	0.29
Zn_7O_7	4.11	5.30	1.19	4.74	0.63	$Zn_{15}O_{15}$	3.56	4.47	0.91	3.90	0.34
	5.06	6.34	1.28	5.78	0.72		3.67	4.54	0.87	3.98	0.31
	5.18	6.21	1.03	5.65	0.47		4.16	4.73	0.57	4.43	0.27
Zn_8O_8	3.24	4.26	1.02	3.69	0.45						
	3.77	4.83	1.06	4.24	0.47						
	4.05	5.07	1.02	4.48	0.43						

[a] D1 ($\Delta E(2) - \Delta E(1)$) and D2 ($\Delta E(3) - \Delta E(1)$) denote the differences between MPW1PW91 and B3LYP with respect to TDDFT, respectively. All energies are in eV.

Inspection of Table 5 reveals that B3LYP yields better results than MPW1PW91, relative to the TDDFT excitation energies. The difference between B3LYP and TDDFT (D2 column) is much smaller than the difference between MPW1PW91 and TDDFT (D1 column).This is due to the fact that the B3LYP HOMO and LUMO lie higher and lower, respectively, than their corresponding MPW1PW91 ones. Analyzing the results closer, we observed that as the cluster size increases the relative differences D1 and D2 decrease. D1 and D2 are smaller for 3D structures than they are for ring structures. Let us now see more carefully the D1 and D2 results.

In the case of D1, it is seen that the values are always greater than 1 eV, but as the cluster size increases, the difference becomes smaller, and is smaller than 1 eV for $Zn_{15}O_{15}$. Nevertheless, the descent is gradual and does not have large oscillations.

The analysis is similar for D2. Ringlike clusters have values larger than 0.5 eV, the values being closer to 0.5 as the cluster size increases. For 3D clusters, these differences are smaller than 0.5 eV. It is observed that these values become smaller and smaller as cluster size increases, and in $Zn_{15}O_{15}$, the values are smaller than 0.40 eV. This is an important point because it provides reasonable approximate excitation energies for large clusters, where TDDFT calculations are prohibitively expensive.

4. Conclusions

TDDFT calculations yield interesting results for the excitation energies of Zn_iO_i clusters. The calculated electronic excitation energies show a strong dependence on the geometry of the cluster. Our study reveals that ringlike structure clusters, $i = 2-7$, have excitation energies larger than those of three-dimensional spheroidal clusters, $i \geq 8$. For both types of clusters, the excitations occur from occupied nonbonding p-type orbitals of oxygen to the LUMO, the different orientation of these orbitals in each structure family being the cause of the difference in ΔE.

The predicted electronic excitation energies of the spheroid clusters lie near the range of the visible spectrum and are close to the experimental absorption energies of small nanoparticles. $Zn_{12}O_{12}$, the most spheroidal cluster, is predicted to have an excitation energy of 3.8 eV, which matches that measured for small ZnO nanocrystals. This led us to hypothesize that the surface structure of these small ZnO nanocrystals might have the $Zn_{12}O_{12}$ cluster's surface pattern. Analysis of the preedge signals of the X-ray absorption spectra of the nanocrystals could validate this model.

The difference between the B3LYP Kohn−Sham energies of the orbitals involved in the sought electronic excitation appears to be a reliable practical approach to the prediction of the electronic excitation energies for larger clusters, where TDDFT calculations become prohibitive. The results calculated with this approach give eigenvalues which, consistent with the TDDFT excitation energies, increase as the cluster size increases. Nevertheless, its most salient drawback is that no oscillator strengths are obtained.

Acknowledgment. This research was funded by Euskal Herriko Unibertsitatea (the University of the Basque Country), Gipuzkoako Foru Aldundia (the Provincial Government of Gipuzkoa), and Eusko Jaurlaritza (the Basque Government).

Supporting Information Available: Experimental tables (PDF). This material is available free of charge via the Internet at http://pubs.acs.org.

JA0264504